Cover Page

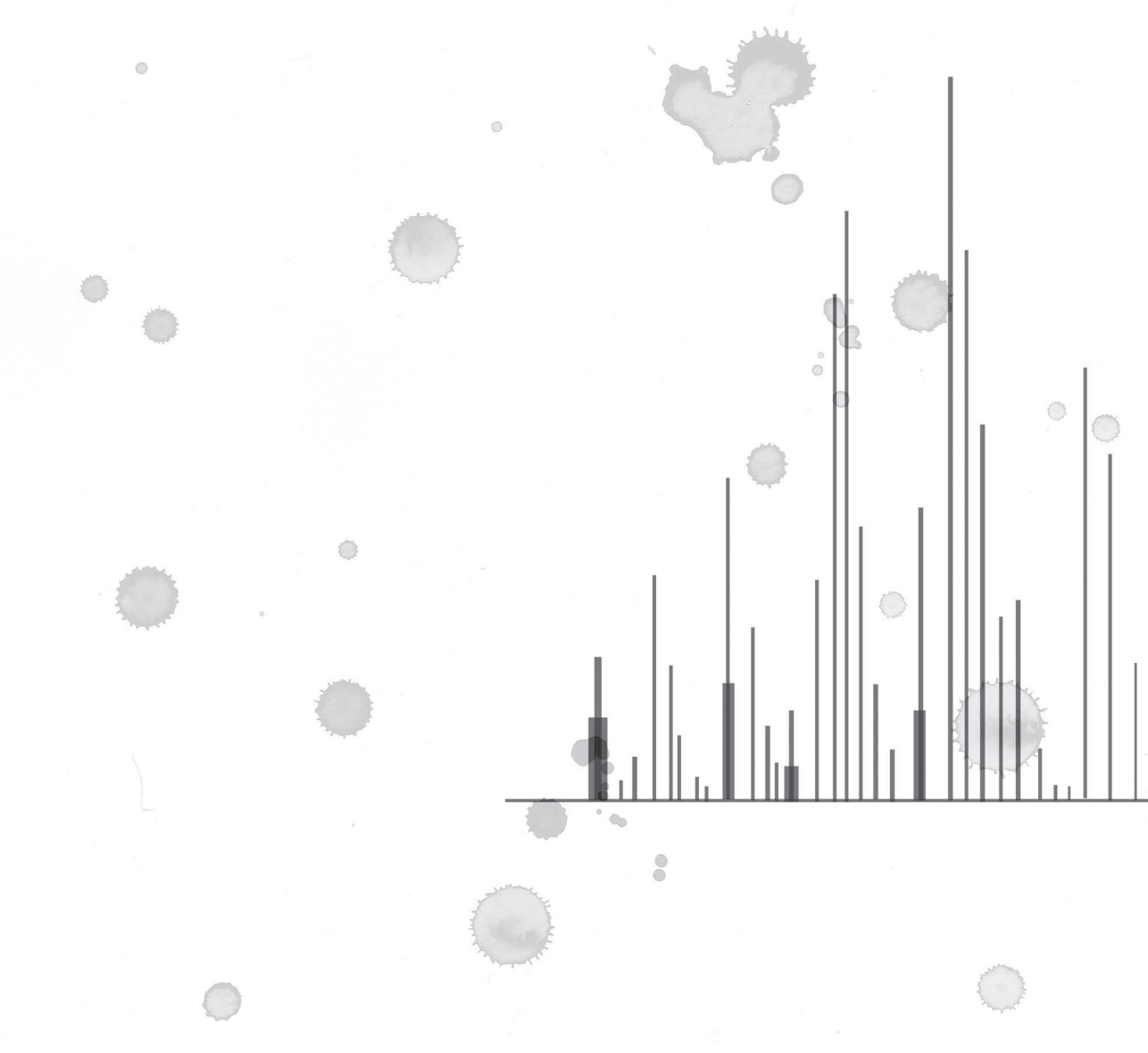The handle http://hdl.handle.net/1887/35155 holds various files of this Leiden University dissertation.

Author: Hussaarts, Leonie
Title: Immune modulation by schistosomes : mechanisms of T helper 2 polarization and implications for metabolic disorders
Issue Date: 2015-09-10

ANALYSIS OF HUMAN DENDRITIC CELL MATURATION AND POLARIZATION USING LABEL-FREE QUANTITATIVE PROTEOMICS

Leonie Hussaarts, Maria Kaisar, Arzu Tugce Guler,
Hans Dalebout, André M. Deelder, Magnus Palmblad
and Maria Yazdanbakhsh

4

ABSTRACT

Dendritic cells (DC) are the sentinels of the immune system. Upon recognition of a pathogen, they undergo maturation and migrate to the lymph node to polarize T helper (Th) subsets. Although it is known that helminths and helminth-derived molecules condition dendritic cells to polarize T cells towards Th2, the underlying mechanism remains unknown. We chose to conduct a proteome analysis of the dendritic cells, in order to gain more insight into the cellular processes associated with their ability to polarize cellular immune responses. We analyzed DC maturation and polarization in nine different donors and at three different time points, using liquid chromatography and high-resolution Fourier transform ion cyclotron resonance mass spectrometry (LC-FTICRMS) for relative quantitation. We report that lipopolysaccharide-induced maturation had the strongest effect on the DC proteome, and promoted expression of proteins related to metabolic, cellular and immune system processes or transport. LPS-DCs additionally stimulated with IFN-γ, a Th1-inducing stimulus, differentially expressed cytoskeletal proteins and proteins involved in immune regulation, after 6h of stimulation, suggesting that they undergo accelerated maturation. Stimulation of LPS-DCs with omega-1 and SEA strongly increased 60S acidic ribosomal protein P2 (RPLP2). In addition, both SEA and omega-1 decreased expression of proteins related to antigen processing and presentation. In conclusion, our data support the hypothesis that reduced interaction between T cells and DCs at the level of the immunological synapse may promote Th2 polarization, and provide novel leads for the identification of molecular mechanisms for Th2 polarization.

INTRODUCTION

Dendritic cells (DCs) (1) are professional antigen-presenting cells located in peripheral tissues, that continuously sample the environment to capture antigens from invading microbes. Upon recognition of pathogens-associated molecules, DCs undergo maturation and migrate to the draining lymph nodes where they present antigen to antigen-specific T helper (Th) cells. Different classes of pathogens polarize DCs for the induction of different types of Th cell responses. In general, rapidly replicating intracellular microorganisms such viruses and certain bacteria activate Th1 cells. The principal regulators of anti-helminth immunity are Th2 cells, and fungi and extracellular bacteria give Th17 responses (2-4).

While much is known about the regulation of Th1 and Th17 responses, the mechanisms that control Th2 activation are still not fully understood (5). Although helminths are strong inducers of Th2 responses, it proved difficult to pinpoint the specific mechanisms involved due to the complex nature of many helminth-derived antigen preparations. For example, *Schistosoma mansoni* soluble egg antigen (SEA), among the most widely used preparations for studying immune responses to helminth antigens, contains more than 600 different proteins (6). The identification of omega-1 as the major immunomodulatory component in SEA therefore provided an opportunity to further dissect the molecular mechanisms underlying Th2 skewing (7;8). We have previously shown that omega-1 is a glycosylated T2 RNase that conditions DCs for Th2 induction by suppressing protein synthesis (9). However, it remains unclear which mechanisms subsequently enable Th2 skewing.

Maturation of DCs is largely controlled at the posttranscriptional and posttranslational level (10;11). Therefore, as a representative indicator of cell function and phenotype, various groups have studied the proteome of pro-Th2 DCs. Using semi-quantitative gel-based techniques, three cytoplasmic proteins were found to be exclusive to the Th2-inducing proteome of human monocyte-derived DCs (12). In mouse bone marrow-derived DCs (BMDCs), four proteins were significantly affected by stimulation with helminth antigens (13). A third study on pro-Th2 BMDCs used iTRAQ labeling for relative quantitation of plasma membrane proteins, and showed that pro-Th2 BMDCs upregulated proteins related to cell metabolism and downregulated proteins associated with the cytoskeleton (14). Although these studies provide valuable directions for future research, the use of 2-DE and iTRAQ does not allow for high-throughput analysis and direct comparison of a large number of biological replicates. This is especially relevant when donor-to-donor variation is expected, for example when working with DCs from human donors, and may explain why only very few proteins were found in common between different gel-based studies on lipopolysaccharide (LPS)-matured human DCs (15-18).

As such, the introduction of a high-resolution label-free and gel-free method for quantitative analysis of DC proteomes would be highly beneficial. In this study, we analyzed DC maturation and polarization using liquid chromatography Fourier transform ion cyclotron resonance mass spectrometry (LC-FTICRMS) for accurate mass measurement and relative quantitation (19;20). This method allowed us to include a total of nine DC donors and four

different stimuli. We included an early (6h) and a late (32h) time point in addition to baseline (0h), to reflect maturation stages associated with migration and antigen presentation. Using SEA, a complex antigen preparation, and omega-1, a single molecule for Th2 polarization, we focus on the identification of proteins associated with the pro-Th2 DC proteome.

RESULTS

Functional characterization of human DCs

Immature DCs (iDCs) generated from nine donors were matured with LPS, in the presence or absence of IFN-γ as a Th1-inducing stimulus, and SEA or omega-1 as Th2-inducing conditions. To functionally characterize these DCs, a co-culture system of human LPS-matured DCs and allogeneic naïve CD4$^+$ T cells was used. DCs expressed high levels of CD1a and no CD14, as expected (**Fig. 1A**), and strongly upregulated CD86 expression upon LPS stimulation (**Fig. 1B**). Additional stimulation with IFN-γ did not affect LPS-induced CD86 expression but strongly induced IL-12p70 production (**Fig. 1C**), while SEA and ω-1 decreased expression of both CD86 and IL-12p70, as described previously (9). Analysis of T cell cytokine production confirmed that omega-1 and SEA induced a Th2 response, characterized by a high frequency of IL-4-producing T cells (**Fig. 1D**), while stimulation of DCs with IFN-γ promoted a Th1 response (**Fig. 1E**).

Protein Identifications

To establish the effect of maturation and polarization on the DC proteome, iDCs and LPS-matured DCs stimulated with IFN-γ, SEA or omega-1, were collected from each of the nine
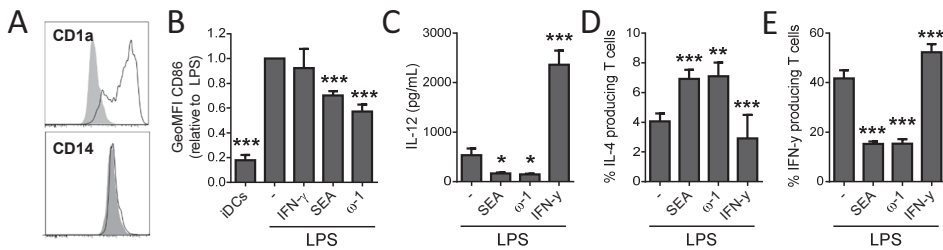

Figure 1. Functional characterization of pro-Th1 and pro-Th2 DCs. Monocyte-derived DCs were either left untreated or pulsed with LPS in the presence or absence of IFN-γ, SEA, or omega-1. After 48h, expression of surface markers was analyzed by flow cytometry. (A) Representative histograms for expression of CD1a and CD14 are shown. Filled histograms represent unstained controls. (B) Expression levels of CD86, based on the geometric mean fluorescence, are shown relative to LPS, which was set to 1. (C) Following stimulation, moDCs were co-cultured with a CD40L-expressing cell line. Supernatants were collected after 24 h and IL-12p70 concentrations were determined by ELISA. (D) 48h-matured DCs were cultured with allogeneic naive CD4$^+$ T cells for 11 days. Intracellular cytokine production as analyzed by flow cytometry after 6h of stimulation with phorbol myristate acetate and ionomycin. The percentages of T cells uniquely positive for either IL-4 or (E) IFN-γ are shown. Bars represent mean values + s.e.m.; *P<0.05; **P<0.01; ***<0.001 for significant differences with the LPS control based on a paired Student's t-test. ω-1, omega-1.

donors at three different time points: before stimulation (0h), six hours after stimulation (6h) and 32 hours after stimulation (32h). Proteins were digested after which peptides were identified using LC-MS/MS in an ion trap, resulting in the identification of 1159 unique peptides from 439 unique proteins with a false-discovery rate (FDR) of 1.0%. These were used for matching with and querying the LC-FTICRMS data for label-free quantitation (19;20). In total, 208 proteins were quantified with multiple peptides in each biological replicate and at each time point.

Effects of maturation on the human DC proteome

To identify proteins that were differentially expressed due to stimulation, the stimulus-induced fold change in abundance was determined for each protein, by calculating the mean fold change of the nine donors. Corresponding p-values were obtained from a paired Student's t-test after log-transformation. Proteins were considered differentially expressed when P<0.05 and the stimulus-induced fold change was more than 1.5-fold decreased or increased (i.e. fold change <0.67 or >1.5). LPS-induced maturation displayed a pronounced effect on the DC proteome. Compared to iDCs, LPS promoted differential expression of ten proteins after 6h (**Table 1**). Analysis of protein classification according to Gene Ontology terms indicated that the eight upregulated proteins are mostly involved in transport or cell communication. The two downregulated proteins were both cytoskeletal proteins. After 32 hours, LPS promoted differential expression of 22 proteins (**Table 1**). The majority of proteins was upregulated and related to different metabolic, cellular and immune system processes or transport. The protein most strongly upregulated by LPS stimulation was TNF receptor-associated factor 1 (TRAF1), an adapter molecule that regulates activation of NF-κB and JNK. In addition, actin cross-linking proteins Fascin and Myristoylated alanine-rich C-kinase substrate (MARCS) were profoundly induced, as well as the MHC class I molecule HLA-B, involved in antigen presentation. Among the four downregulated proteins, Macrophage mannose receptor 1 is involved in antigen uptake, cathepsins play a role in antigen processing, and Ganglioside GM2 activator (GM2A) mediates presentation of lipids (21-23).

Effects of polarizing stimuli on the human DC proteome

LPS-matured DCs additionally stimulated with IFN-γ, a Th1-inducing stimulus, differentially expressed ten proteins after 6h of stimulation compared to stimulation with LPS alone (**Table 2**). Five proteins were downregulated, of which three were members of the cytoskeleton. The proteins most strongly upregulated were Heat Shock Protein HSP 90-alpha (HSP90AA1), which mediates inflammatory responses, and cytoplasmic tryptophan--tRNA ligase (WARS), also known as Interferon-induced protein 53. After 32h, four proteins were downregulated (**Table 2**), including a tyrosine-protein kinase involved in regulation of immune responses (FGR), and Peptidyl-prolyl cis-trans isomerase A (PPIA), also known as Cyclophilin A, which plays an important role in protein folding, trafficking, and immune cell activation (24).

Following 6h of stimulation with Th2-inducing SEA, five proteins were upregulated compared to stimulation with LPS alone (**Table 2**). Interestingly, in contrast to 32h of

Table 1. Differentially expressed proteins in LPS-DCs versus iDCs.

Accession	Protein	6 hours		32 hours	
		Fold	P-val	Fold	P-val
LPS-induced, 6 hours					
P45880	Voltage-dependent anion-selective channel protein 2	2.74	**0.04**	1.81	0.57
P30040	Endoplasmic reticulum resident protein 29	2.59	**0.00**	1.67	0.64
Q13077	TNF receptor-associated factor 1	2.25	**0.01**	14.95	**0.00**
P61604	10 kDa heat shock protein. mitochondrial	2.23	**0.03**	1.68	0.76
P05362	Intercellular adhesion molecule 1	1.89	**0.00**	3.60	**0.01**
P30464*	HLA class I histocompatibility antigen, B-15 alpha chain	1.83	**0.02**	7.89	**0.00**
P29966	Myristoylated alanine-rich C-kinase substrate	1.77	**0.02**	10.76	**0.00**
Q9BQE5	Apolipoprotein L2	1.64	**0.05**	2.95	**0.00**
Q71U36	Tubulin alpha-1A chain	0.63	**0.03**	1.58	0.82
P06396	Gelsolin	0.62	**0.00**	1.96	0.48
LPS-induced, 32 hours					
Q13077	TNF receptor-associated factor 1	2.25	**0.01**	14.95	**0.00**
P29966	Myristoylated alanine-rich C-kinase substrate	1.77	**0.02**	10.76	**0.00**
P30464*	HLA class I histocompatibility antigen, B-15 alpha chain	1.83	**0.02**	7.89	**0.00**
Q16658	Fascin	1.26	0.61	5.48	**0.00**
P04179	Superoxide dismutase [Mn], mitochondrial	1.20	0.68	4.66	**0.00**
P23381	Tryptophan--tRNA ligase, cytoplasmic	0.98	0.55	3.77	**0.00**
Q9UL46	Proteasome activator complex subunit 2	0.92	0.25	3.68	**0.00**
P05362	Intercellular adhesion molecule 1	1.89	**0.00**	3.60	**0.01**
P80723	Brain acid soluble protein 1	1.21	0.54	3.46	**0.00**
P27348	14-3-3 protein theta	0.96	0.40	3.00	**0.00**
Q9BQE5	Apolipoprotein L2	1.64	0.05	2.95	**0.00**
P19971	Thymidine phosphorylase	1.00	0.76	2.79	**0.04**
Q14974	Importin subunit beta-1	0.98	0.38	2.39	**0.02**
P02786	Transferrin receptor protein 1	1.14	0.77	2.20	**0.00**
P08107	Heat shock 70 kDa protein 1A/1B	1.19	0.41	1.93	**0.02**
P20700	Lamin-B1	1.34	0.40	1.85	**0.04**
P34931	Heat shock 70 kDa protein 1-like	1.16	0.52	1.55	**0.04**
Q9BZQ8	Protein Niban	1.14	0.32	1.54	**0.01**
P07339	Cathepsin D	1.68	0.76	0.63	**0.03**
P22897	Macrophage mannose receptor 1	0.98	0.36	0.63	**0.02**
P17900	Ganglioside GM2 activator	1.40	0.19	0.58	**0.02**
Q9UBR2	Cathepsin Z	1.30	**0.01**	0.56	**0.00**

*HLA serotypes originate from the same gene and share common peptides. The serotype attributed to the identification may therefore not be accurate.

4

stimulation with IFN-γ, SEA induced strong upregulation of PPIA. SEA also increased expression of Eukaryotic initiation factor 4A-I, involved in translation initiation, Endoplasmin (HSP90B1), HSP90AA1, and Fascin. After 32h, SEA promoted differential expression of six proteins (**Table 2**). Among those, four proteins were downregulated, including WARS which was induced by IFN-γ, and HLA-B and CD44 which are involved in antigen presentation and T cell activation (25). The protein most strongly upregulated by 32h of SEA stimulation was 60S acidic ribosomal protein P2 (RPLP2), which plays an important role in the elongation step of protein synthesis.

Omega-1 induced upregulation of five proteins after 6h, and seven proteins after 32 hours (**Table 2**), most of which were ribosomal proteins, chaperones or enzymes. Among those, several proteins were highly upregulated, including mitochondrial Thioredoxin-dependent peroxide reductase (6h), a protein involved in redox regulation of the cell, RPLP2 (32h), and the chaperone Calnexin (32h). After 32h of omega-1 stimulation, seven proteins were downregulated. In particular, omega-1 strongly decreased expression of HLA-B, HLA-C and CD44, as well as MARCS.

Analysis of proteins exclusive to the Th2-inducing proteome

The identification of proteins uniquely associated with the Th2-inducing DC proteome could provide valuable leads for understanding initiation of Th2 responses by DCs. We therefore analyzed proteins affected by stimulation with SEA as well as omega-1, by looking at protein expression dynamics and individual donor responses. As can be appreciated from **Table 2**, omega-1 and SEA did not share differentially expressed proteins after 6h of stimulation. After 32h, however, they shared five differentially expressed proteins. Among those five, Transferrin receptor protein 1 is seemingly downregulated by omega-1 and SEA, but also by IFN-γ (P=0.051), suggesting that this may not be a Th2-exclusive protein.

Analysis of protein expression dynamics of the four remaining Th2-associated proteins showed that RPLP2 was strongly upregulated by 32h of stimulation with SEA and omega-1 in at least eight out of nine donors (**Fig. 2A**). Synaptic vesicle membrane protein VAT-1 homolog (VAT1) was upregulated by SEA and omega-1 in at least seven donors after 32h of stimulation (**Fig. 2B**), but was also mildly increased by IFN-γ stimulation in the majority of donors. CD44 was significantly downregulated by SEA in seven donors, and by omega-1 nine donors (**Fig. 2C**). Lastly, LPS-induced upregulation of HLA-B was inhibited by SEA and omega-1 in eight donors (**Fig. 2D**). These findings suggest that in particular upregulation of RPLP2, and downregulation of CD44 and HLA-B, are characteristics of pro-Th2 DCs.

Further exploration of the data by association analysis

To explore whether there are specific networks and functional classifications significantly affected by Th2-inducing stimuli, we analyzed our data using GeneMANIA software. For hypothesis-generating purposes, less stringent thresholds were applied. First, all proteins significantly affected by stimulation (i.e. fold change P<0.05); and second, those proteins with P<0.1 and a fold change of <0.67 or >1.5, were included. For a complete list of all accessions (with

Table 2. Differentially expressed proteins in pro-Th1 and pro-Th2 DCs versus LPS-DCs.

Accession	Protein	IFN-γ		SEA		Omega-1	
		Fold	P-val	Fold	P-val	Fold	P-val
IFN-γ-induced, 6 hours							
P07900	Heat shock protein HSP 90-alpha	2.42	**0.02**	2.98	**0.02**	2.42	0.14
P23381	Tryptophan--tRNA ligase, cytoplasmic	2.13	**0.04**	1.20	0.43	1.07	0.61
P13639	Elongation factor 2	1.82	**0.01**	1.64	0.12	1.34	0.33
P30508*	HLA class I histocompatibility antigen, Cw-12 alpha chain	1.78	**0.03**	1.61	0.41	1.29	0.97
P09467	Fructose-1.6-bisphosphatase 1	1.69	**0.02**	1.54	0.07	1.53	0.25
P26038	Moesin	0.66	**0.04**	0.86	0.16	1.12	0.58
P67936	Tropomyosin alpha-4 chain	0.66	**0.02**	0.90	0.18	1.08	0.36
P02545	Prelamin-A/C	0.64	**0.00**	0.95	0.21	1.09	0.73
P16070	CD44 antigen	0.63	**0.01**	1.01	0.40	0.89	0.21
P10599	Thioredoxin	0.52	**0.02**	2.31	0.33	1.10	0.07
IFN-γ-induced, 32 hours							
P40926	Malate dehydrogenase. mitochondrial	0.59	**0.00**	0.99	0.29	0.97	0.38
P62937	Peptidyl-prolyl cis-trans isomerase A	0.58	**0.02**	2.38	0.44	3.71	0.59
P04908	Histone H2A type 1-B/E	0.55	**0.00**	1.07	0.15	1.31	0.20
P09769	Tyrosine-protein kinase Fgr	0.65	**0.03**	0.68	**0.01**	0.95	0.40
SEA-induced, 6 hours							
P62937	Peptidyl-prolyl cis-trans isomerase A	4.02	0.45	11.27	**0.01**	1.62	0.54
Q9BZQ8**	Protein Niban	1.10	0.85	9.78	**0.00**	1.03	0.89
P14625	Endoplasmin	1.47	0.58	4.14	**0.04**	2.31	0.88
P60842	Eukaryotic initiation factor 4A-I	1.83	0.32	3.21	**0.04**	1.17	0.47
P07900	Heat shock protein HSP 90-alpha	2.42	**0.02**	2.98	**0.02**	2.42	0.14
Q16658	Fascin	1.15	0.92	1.74	**0.04**	1.40	0.32
SEA-induced, 32 hours							
P05387	60S acidic ribosomal protein P2	1.68	0.17	2.27	**0.01**	4.63	**0.01**
Q9BZQ8**	Protein Niban	1.19	0.20	2.20	**0.01**	1.20	0.73
Q99536	Synaptic vesicle membrane protein VAT-1 homolog	1.29	0.20	1.59	**0.03**	1.53	**0.02**
P16070	CD44 antigen	1.47	0.81	0.63	**0.02**	0.47	**0.00**
P23381	Tryptophan--tRNA ligase, cytoplasmic	1.45	0.34	0.60	**0.00**	0.92	0.19
P02786	Transferrin receptor protein 1	0.75	0.05	0.56	**0.00**	0.49	**0.00**
P30464*	HLA class I histocompatibility antigen, B-15 alpha chain	1.27	0.79	0.45	**0.00**	0.40	**0.00**
Omega-1-induced, 6 hours							
P30048	Thioredoxin-dependent peroxide reductase, mitochondrial	7.06	0.14	2.56	0.64	4.03	**0.04**
P05388	60S acidic ribosomal protein P0	1.47	0.06	1.31	0.64	1.86	**0.02**
P30041	Peroxiredoxin-6	1.33	0.63	1.44	0.33	1.77	**0.02**
Q01813	6-phosphofructokinase type C	1.39	**0.02**	1.13	0.43	1.65	**0.01**
P61158	Actin-related protein 3	1.47	0.50	2.11	0.67	1.61	**0.04**

Table 2. Differentially expressed proteins in pro-Th1 and pro-Th2 DCs versus LPS-DCs. (*Continued*)

Accession	Protein	IFN-γ		SEA		Omega-1	
		Fold	P-val	Fold	P-val	Fold	P-val
Omega-1-induced, 32 hours							
P05387	60S acidic ribosomal protein P2	1.68	0.17	2.27	**0.01**	4.63	**0.01**
P27824	Calnexin	1.32	0.93	1.76	0.51	2.64	**0.05**
P55084	Trifunctional enzyme subunit beta, mitochondrial	1.72	0.14	1.48	0.13	2.52	**0.05**
P63104	14-3-3 protein zeta/delta	1.60	0.55	1.51	0.18	2.33	**0.04**
P50502	Hsc70-interacting protein	1.29	0.48	1.45	0.06	2.05	**0.02**
P30041	Peroxiredoxin-6	0.94	0.32	1.46	0.32	2.02	**0.02**
Q99536	Synaptic vesicle membrane protein VAT-1 homolog	1.29	0.20	1.59	**0.03**	1.53	**0.02**
P17900	Ganglioside GM2 activator	1.04	0.20	1.26	0.68	0.65	**0.03**
P30508	HLA class I histocompatibility antigen, Cw-12 alpha chain	1.02	0.29	1.01	0.05	0.63	**0.01**
P29966	Myristoylated alanine-rich C-kinase substrate	1.19	0.78	0.73	0.06	0.58	**0.01**
P04179	Superoxide dismutase [Mn]. mitochondrial	1.30	0.85	1.24	0.37	0.52	**0.01**
P02786	Transferrin receptor protein 1	0.75	0.05	0.56	**0.00**	0.49	**0.00**
P16070	CD44 antigen	1.47	0.81	0.63	**0.02**	0.47	**0.00**
P30504*	HLA class I histocompatibility antigen, Cw-4 alpha chain	0.72	0.10	1.88	0.21	0.47	**0.02**
P30464*	HLA class I histocompatibility antigen, B-15 alpha chain	1.27	0.79	0.45	**0.00**	0.40	**0.00**

*HLA serotypes originate from the same gene and share common peptides. The serotype attributed to the identification may therefore not be accurate.**The signal attributed to the VLTSEDEYNLLSDR peptide in NIBAN is likely coming from the $^{13}C_1$-peak of the YCLQLYDETYER peptide from the SEA-derived protein Interleukin-4-inducing protein (IPSE). Protein Niban was removed from further analysis.

corresponding gene names) included for GeneMANIA analysis, see **Table S1**. In addition to the genes of the differentially expressed proteins, we allowed for display of ten associated genes.

After 6h of stimulation, SEA promoted differential expression of proteins in a network enriched for mitochondrial matrix proteins (FDR = 0.055) and MHC class II protein complex binding (FDR = 0.002) (**Fig. S1**). The two SEA-responsive proteins involved in MHC class II protein complex binding were the MHC class II molecule HLA-DRA and Heat Shock Protein HSP90AA1, which were increased by SEA treatment (**Table S1**). By contrast, after 32h of treatment, SEA decreased expression of HLA-DRB1, another MHC class II molecule, in line with previous studies on long-term SEA treatment of DCs (26). GeneMANIA analysis indicated that 32h of SEA treatment affected proteins in a network enriched for antigen processing and presentation (FDR = 0.001) (**Fig. S2**). Examination of the three SEA-responsive proteins within this functional classification indicated that all three proteins (HLA-B, HLA-DRB1 and CD74) were downregulated.

Stimulation with omega-1 induced differential expression of proteins in a network enriched for phagocytosis (FDR = 0.000, proteins were both up- and downregulated) and glycolysis (FDR = 0.039) (Fig. S3). Related to glycolysis, omega-1 increased expression of 6-phosphofructokinase
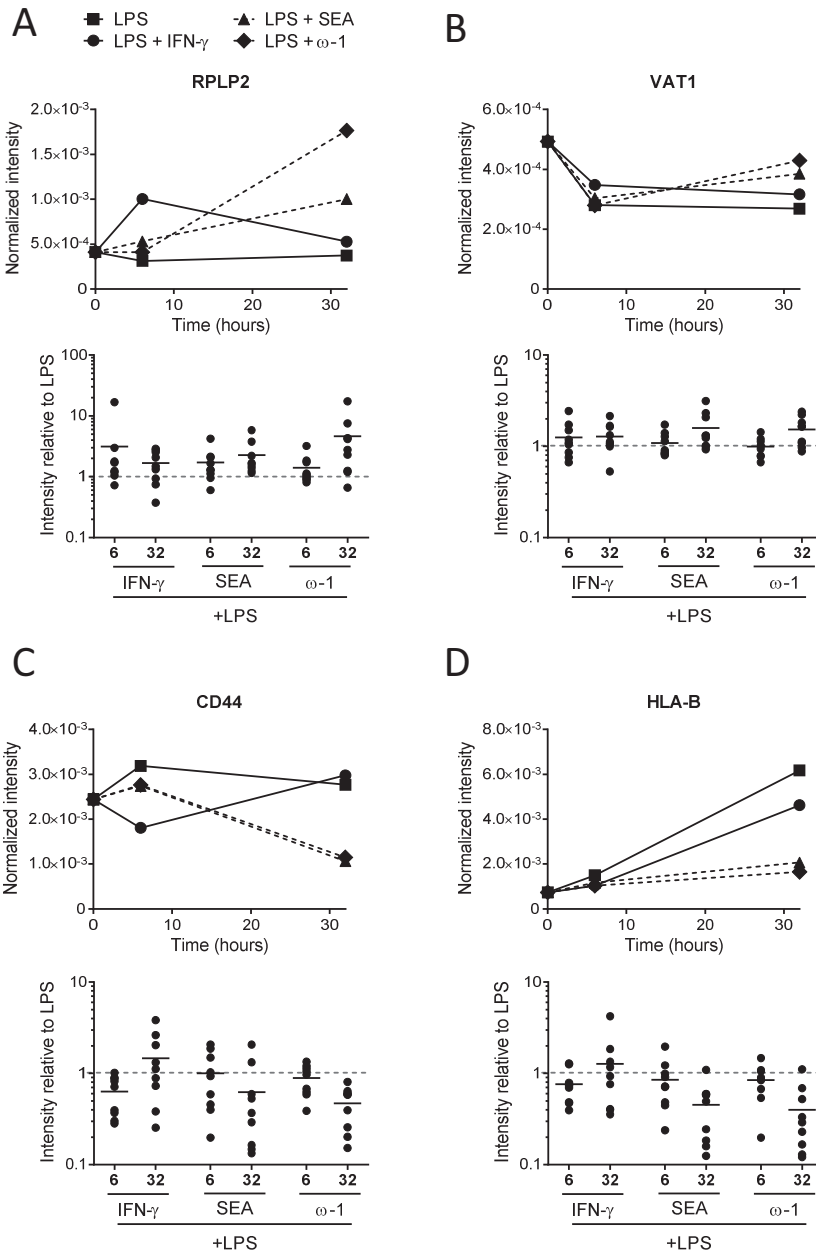
Figure 2. Protein expression dynamics of Th2-associated differentially expressed proteins. Monocyte-derived DCs were stimulated as described in the legend of figure 1. Protein expression was analyzed by LC-FTICRMS. Differentially expressed proteins shared between 32h of stimulation of with omega-1 and SEA are shown. The top panel of each figure shows the protein expression dynamics, the bottom panel shows the normalized intensity relative to LPS, which was set to 1 at 6h and at 32h (dashed line). (A) 60S acidic ribosomal protein P2. (B) Synaptic vesicle membrane protein VAT-1 homolog. (C) CD44 antigen. (D) HLA-B.

type C (PFKP), which catalyzes the third step of glycolysis, while expression of Glyceraldehyde 3-phosphate dehydrogenase (GAPDH) that catalyzes the sixth step was decreased (Table S1). Like SEA, 32h of omega-1 treatment affected proteins in a network enriched for antigen processing and presentation (FDR = 0.000; Fig. 3). Out of the four omega-1-responsive proteins within this functional classification, three were downregulated (HLA-B, HLA-C and Cathepsin D). In addition, 32h of omega-1 stimulation affected proteins in a network significantly enriched for translational elongation (FDR = 0.001). Within this functional classification, RPLP2 and Elongation factor 1-delta (EEF1D) were upregulated, while Ubiquitin-60S ribosomal protein L40 (UBA52) was downregulated.
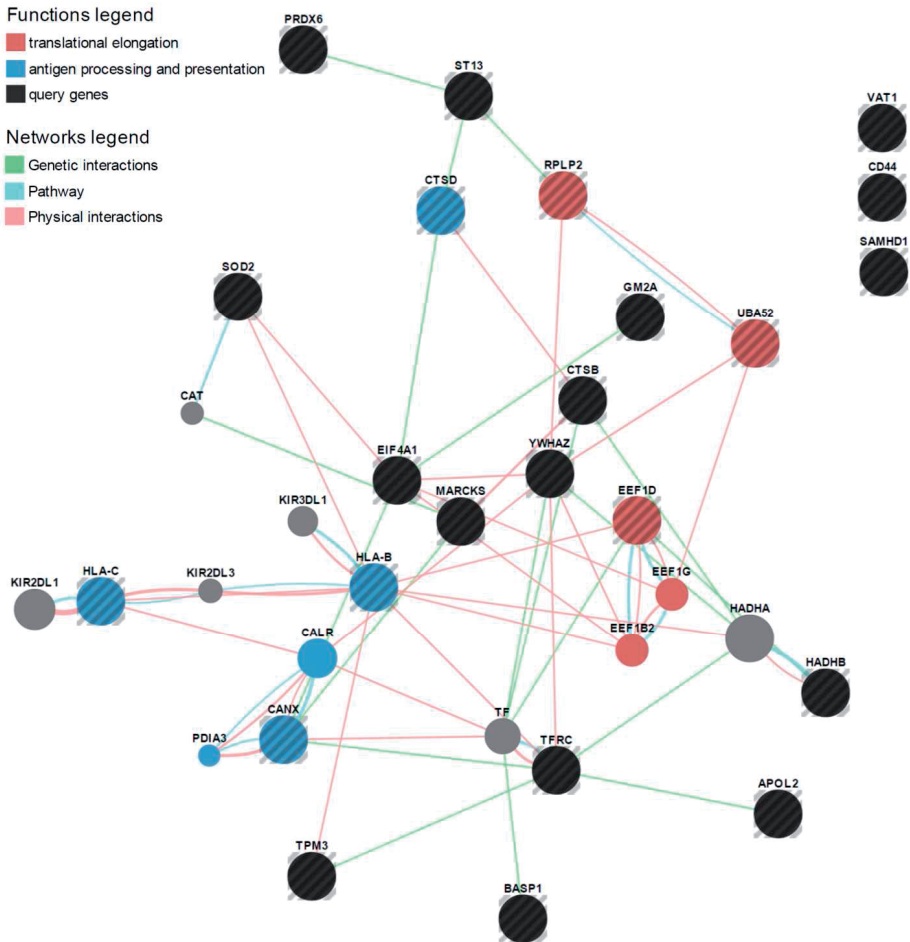
4

Figure 3. Network analysis of 32h omega-1-response proteins. Monocyte-derived DCs were stimulated as described for the legend of figure 1, and protein expression was analyzed by LC-FTICRMS. For GeneMANIA analysis, all 32h omega-1-responsive proteins with P<0.05, and those proteins with P<0.1 and a fold change of <0.67 or >1.5, were included. Black and/or striped nodes represent genes of which the proteins were differentially expressed (query genes); grey nodes represent associated genes added by GeneMANIA. Colored nodes highlight significantly enriched Gene Ontologies.

DISCUSSION

Over the past decade, studies on the proteome of matured or polarized DCs relied on label- and gel-based techniques. Such approaches do not allow for high-throughput analysis of many different conditions or biological replicates, which might explain why only few proteins were found in common between different reports (15-18;27). Here, we used ion traps for tandem mass spectrometry and LC-FTICRMS for label- and gel-free quantitation (19), which had previously been used for the analysis of the plasma proteome (20). This approach allowed us to analyze the proteomes of LPS-matured and pro-Th1 versus pro-Th2 DCs from nine different human donors.

As expected, LPS-induced maturation displayed the most pronounced effect on the DC proteome. After 6h of maturation, proteins involved in intracellular transport and cell communication were upregulated, and cytoskeletal proteins were either up- or downregulated. These processes may reflect that the DCs are preparing for migration, which requires profound alterations in cell morphology and motility (28). The strongest effect on the DC proteome was observed after 32h of LPS-induced maturation, when many proteins were upregulated at least 3-fold. Among the proteins most strongly induced was mitochondrial Superoxide dismutase (SODM). Indeed, DCs are known to upregulate reactive oxygen species in response to stimulation with LPS (29;30), and subsequent upregulation of superoxide dismutases has also been reported (31). In addition, stimulation with LPS induced Fascin, an actin cross-linking that plays a critical role in migration of mature DCs into lymph nodes. Specifically, actin bundling by Fascin was shown to promote membrane protrusions and mediates disassembly of podosomes, which are specialized structures for cell-matrix adhesion (32). A second actin cross-linking protein, MARCS, was also profoundly induced, in line with a previous report (33). The other two proteins most strongly affected by LPS stimulation were MHC class I molecule HLA-B, involved in antigen presentation, and TRAF1, an adapter molecule that regulates activation of NF-κB and JNK. Indeed, NF-κB activation was previously shown to be required for DC maturation (34). The proteins downregulated after 32h of LPS stimulation were involved in antigen uptake, processing and presentation of lipids. Together, these findings reflect that after 32h of stimulation, LPS-DCs have become specialized for entering lymph nodes and presenting antigen to naïve T cells, which identifies the FTICR-ion trap cluster as an appropriate method to for high-throughput quantitative analysis of dendritic cell lysates.

Importantly, we find many differentially expressed proteins in common with a proteomics study by Ferreira *et al.* (35), which further validates our method. In our and their study, maturation reduces expression of cathepsins and GM2A, and increases expression of Apolipoprotein L2, Fascin, Proteasome activator complex subunit 2, and SODM. Furthermore, in line with another report (11), we observe an increase in Heath shock protein (Hsp) expression. Unique to our study, the FTICR method allowed us to perform statistical analysis on protein expression data from nine biological replicates. In addition, multiple time points were included, which provides information about protein expression dynamics. Our study therefore strengthens and expands previous reports on maturation of human DCs.

4

Using the cytokine IFN-γ, we polarized LPS-DCs for Th1 skewing, and observed that pro-Th1 DCs differentially expressed cytoskeletal proteins and proteins involved in inflammatory processes after 6h of stimulation, compared to LPS-DCs. Among those proteins, HSP90AA1 and WARS were most strongly upregulated. Indeed, under inflammatory conditions, heat shock proteins (HSPs) can act as chaperones to facilitate antigen presentation and enhance the immune response (36). In line with our results, Ferreira *et al.* also described upregulation of WARS in DCs following LPS + IFN-γ treatment (35). It has been demonstrated that transcription of WARS is responsive to IFN-γ treatment in in non-lymphoid cell lines (37), and tryptophan catabolism was shown to promote DC-mediated T cell tolerance (38), but role of WARS in DC-mediated T cell activation remains to be determined. After 32h of IFN-γ stimulation, the effect on the DC proteome was less pronounced, as only 4 proteins were downregulated, including FGR and PPIA involved in immune regulation and activation. These findings may suggest that IFN-γ treatment induces strong effects early after treatment, reminiscent of accelerated maturation.

Interestingly, in contrast to 32h of treatment with IFN-γ, short-term (6h) stimulation of DCs with Th2-inducing SEA induced strong expression of PPIA, also known as Cyclophilin A, which is the primary binding protein of Cyclosporin A, an immunosuppressive drug that antagonizes calcium-dependent T cell activation (39). How the the expression of Cyclophilin A affects the polarizing capacity of DCs remains to be investigated.

Since only few proteins were differentially expressed by 6h SEA or omega-1 treatment, we also performed association analysis using GeneMANIA, applying less stringent thresholds for hypothesis generation. SEA induced differential expression of proteins in a network enriched for mitochondrial matrix proteins, and omega-1 affected proteins in a network enriched for glycolysis. Although the differentially expressed proteins within those functional classifications were both up- and down-regulated, these findings may suggest that 6h after stimulation, SEA and omega-1 may affect cellular metabolism. In line with these findings, recent studies have indicated that modulation of metabolic pathways within dendritic cells can regulate DC function and the outcome of the immune response (40;41). Whether omega-1 and SEA indeed modulate cellular metabolism, and whether this contributes to Th2 polarization, requires further studies.

The most profound effect of Th2-inducing stimuli was observed after 32h of stimulation, when SEA and omega-1 both strongly increased expression of ribosomal protein RPLP2. Since the presence of ribosomal P proteins may enhance ribosomal performance (42), we speculate that the increase in RPLP2 may represent a feedback mechanism secondary to SEA- and omega-1-induced ribosome degradation. In addition, SEA and omega-1 decreased expression of CD44 and suppressed LPS-induced upregulation of HLA-B. Interestingly, CD44 expression by DCs was shown to promote CD4 T cell proliferation (25). Together, these findings may suggest that Th2-inducing conditions interfere with efficient antigen presentation to T cells. Indeed, GeneMANIA analysis indicated that SEA and omega-1 both decreased expression of proteins in a protein network enriched for antigen processing and presentation. It has been suggested that T cells are polarized towards Th2 if the interaction between DCs and T cells is weak (43-45).

In addition, it was demonstrated that omega-1 reduces the capacity of bone marrow-derived DCs to form T cell-DC conjugates (8). Taken together, these studies suggest that reduced interaction between T cells and DCs at the level of the immunological synapse may promote Th2 polarization by helminth antigens.

In conclusion, our work has identified the FTICR-ion trap cluster as an appropriate method for quantitative high-throughput analysis of cell lysates. Our data on DC polarization suggest that pro-Th1 DCs undergo accelerated maturation compared to LPS-DCs, and indicate that pro-Th2 DCs may affect cellular metabolism and decrease expression of proteins involved in antigen processing and presentation. Future research should therefore focus on studying the contribution of metabolic pathways, TCR signaling, and the possible relation between the two, to further dissect the mechanisms of helminth-induced T helper 2 polarization via dendritic cells. Such investigations will not only improve our fundamental understanding of DC biology, but may also provide leads for the development of DC-based immunotherapies.

METHODS

Human DC culture, stimulation, and analysis

Monocytes isolated from venous blood of 9 healthy volunteers were differentiated as described previously (46). On day 6 the immature DCs (iDCs) were stimulated with SEA (50 mg/mL), omega-1 (250 ng/mL) or IFN-γ (1000 U/mL) in the presence of 100ng/mL ultrapure LPS (E. coli 0111 B4 strain, InvivoGen) and human rGM-CSF (20 ng/ml;   Life Technologies). At the indicated time points, samples were collected for protein extraction and digestion as described below. Alternatively, after 48 hours of stimulation, expression of surface molecules was determined by flow cytometry (FACSCanto, BD Biosciences) using the following antibodies: CD14 PerCP, CD86 FITC (both BD Biosciences), and CD1a PE (Beckman-Coulter). In addition, $1x10^4$ 48h-matured DCs were co-cultured with $1x10^4$ CD40L-expressing J558 cells. Supernatants were collected after 24h and IL-12p70 concentrations were determined by ELISA using mouse anti-human IL-12 (clone 20C2) as a capture antibody and biotinylated mouse anti-human IL-12 (clone C8.6) as a detection antibody (BD Biosciences). Volunteers signed informed consent forms and the samples were handled according to the guidelines described by the Dutch Federation of Medical Scientific Societies in the Code of Conduct for the responsible use of human tissue for medical research (47).

Human T cell culture and analysis of T cell polarization

For analysis of T cell polarization, $5x10^3$ matured DCs were cultured with $2x10^4$ allogeneic naïve CD4+ T cells that were isolated from buffy coat (Sanquin) peripheral blood mononuclear cells using a CD4+/45RO- Naive T Cell Enrichment Column (R&D Systems). Co-cultures were performed in the presence of staphylococcal enterotoxin B (10 pg/mL). On days 6 and 8, rhuIL-2 (10 U/mL, R&D Systems) was added and the T cells were expanded until day 11. Intracellular cytokine production was analyzed after restimulation with 100 ng/mL phorbol myristate acetate plus 1 µg/mL ionomycin for 6h; 10 µg/mL brefeldin A was added during the last 4h and the cells were fixed with 3.7% paraformaldehyde (all Sigma-Aldrich). The cells were permeabilized with

0.5% saponin (Sigma-Aldrich) and stained with PE- and FITC-labelled antibodies against IL-4 and IFN-γ, respectively (BD Biosciences).

Protein extraction and in-solution digestion

Cells were harvested with PBS at the indicated time points and centrifuged at 522 *g* for 8 minutes at 4°C, after which they were transferred with 1 mL PBS to a microcentrifuge tube and centrifuged for 5 minutes at 5,000 *g,* 4°C. The supernatant was removed and pellets were snap-frozen in liquid nitrogen and stored at -80°C. Samples were thawed in 30 µL lysis buffer consisting of 1% SDS, 125 U/mL benzonase nuclease (Sigma), 2 mM MgCl2, and protease inhibitors (cOmplete ULTRA tablets, mini, EDTA-free, Roche) in 50 mM ammonium biocarbonate (ABC). Samples were placed at 95°C for 5 minutes and following centrifugation at 16 000 *g* for 30 min, the supernatant was collected. A BCA assay (Pierce Biotechnology) was conducted to determine the protein concentration. An equivalent of 10 µg protein was dissolved in 25 µL ABC and reduced using 10 mM DTT (Sigma) for 5 minutes at 95°C, followed by 1 hour alkylation using 40 mM iodoacetamide (Sigma) at room temperature. Using 3 kDa spin filters, the remainder of the lysis buffer was exchanged for ABC according to manufacturer's protocol (Millipore), and samples were digested for 17 hours with sequencing-grade trypsin (Promega) at an enzyme to protein ratio of 1:50. The digestion was quenched with 2% trifluoracetic acid to lower the pH. Peptide samples were stored at -35°C until analysis.

Liquid chromatography - mass spectrometry

All samples were analyzed using a splitless NanoLC-Ultra 2D plus (Eksigent) system for parallel liquid chromatography (LC) with additional trap columns for desalting. The LC systems were configured with 300 µm-i.d. 5-mm PepMap C18 trap columns (Thermo Fisher Scientific) and 15-cm 300 µm-i.d. ChromXP C18 columns (Eksigent). Peptides were separated by a 90-minute linear gradient from 4 to 33% acetonitrile in 0.05% formic acid with the 4 µl/min flow rate. The LC systems were coupled on-line to amaZon speed ETD high-capacity 3D ion traps and a 12 T solariX FTICR system (all from Bruker Daltonics) in an FTICR-ion trap cluster (19). For peptide identification in the ion traps, we generated three sample pools. Pool 1 contained a fraction of each sample that was stimulated for 32h with LPS or LPS + IFN-γ. Pool 2 contained a fraction of each 0h and 6h iDC sample. Pool 3 contained a fraction of each uneven sample (all samples received a random number). These sample pools were run in triplicate on the ion traps. Up to ten abundant multiply charged precursors in *m/z* 300-1300 were selected for MS/MS in each MS scan in a data-dependent manner. After having been selected twice, each precursor was excluded for one minute. The LC systems were controlled using the HyStar 3.4 (Bruker) with a plug-in from Eksigent, the amaZon ion trap by trapControl 7.0, and the solariX FTICR system by solariXcontrol 1.3 (both Bruker).

Data analysis

The raw datasets from ion trap LC-MS/MS and LC-FTICRMS were converted to mzXML (48). The mzXML files were analysed using a scientific workflow called "Label-free proteomics using

LC-MS" (http://www.myexperiment.org/workflows/4552.html). The workflow was designed using the Taverna workflow management system (49).

The LC-MS/MS data was used for identification. The TANDEM application (50) from the X!Tandem provided in Trans Proteomics Pipeline V4.7.7 was run to match the spectra with tryptic peptide sequences derived from UniProt *Homo sapiens* reference proteome database retrieved on 25.07.2014, for each pooled sample. The k-score plug-in was selected for the search with a minimum ion count of 1, and 2 maximum missed cleavage sites. The allowed parent monoisotopic mass error was ±5.0 Da, and the allowed fragment monoisotopic mass error was 0.4 Da. After peptide assignments to MS/MS spectra, the results were converted to pepXML format, an XML-based format that is used in peptide-level analysis (51), using the Tandem2XML application.

To use the high-resolution MS profiles for more precise quantification, each pepXML file was aligned with one master LC-FTICRMS data file. The alignment was done with pepAlign (52), which uses a genetic algorithm to align the two chromatographic time scales with a partial linear function. The output from pepAlign was the breakpoints of this function. The alignment was based on the X! Tandem expect scores and allowed a mass measurement error of ±50 ppm. The retention times in each pepXML file were changed according to the chromatographic alignment function by the pepWarp program. The accuracy of the peptide assignments to tandem mass spectra was assessed by PeptideProphet using the xinteract application provided in Trans Proteomics Pipeline V4.6.3 (53). This application also combined the input datasets, so that all identifications with assigned probabilities were contained in a single output file. This validated pepXML was then aligned with each individual LC-FTICRMS dataset. For quantitation of identified peptides, we used only peptides with PeptideProphet probabilities higher than 0.9369, giving a peptide-spectrum match false discovery rate of 1.0%. Modified peptides were not included.

The monoisotopic mass was calculated for each peptide of interest and the maximum intensity corresponding to this mass was extracted from a window ±60 seconds relative to the aligned retention time and ±25 ppm relative to the calculated mass. As the final output of the workflow, all peptide quantifications were combined into a single table where each row represents a peptide sequence and each column contains the intensity of that peptide in each sample. Missing values were imputed from a normal distribution representing the background signal removed during acquisition. A final matrix was created with proteins identified by more than two peptides, where the abundance of each protein was calculated as the median intensity of its peptides and normalized to the total signal intensity of all proteins in the entire LC-MS dataset. Fold changes in protein abundance between conditions were calculated in R based on the mean fold change of the nine different donors, and corresponding p-values were obtained from paired Student's t-testing of log-transformed protein intensities for each treatment and time point. Analysis of Gene Ontology terms was performed using Protein Annotation THrough Evolutionary Relationship (PANTHER) (54;55), and association analysis was performed using GeneMANIA (56). Associations were analyzed based on genetic interactions, pathways, and physical interactions. In addition to the differentially expressed proteins, we allowed for display of 10 related proteins and 10 related attributes, and Gene Ontology network weighting was based on biological processes.

ACKNOWLEDGEMENTS

REFERENCES

1. Steinman RM, et al. Identification of a novel cell type in peripheral lymphoid organs of mice. I. Morphology, quantitation, tissue distribution. *J Exp Med* 1973 May 1;137(5):1142-62.

2. Kapsenberg ML. Dendritic-cell control of pathogen-driven T-cell polarization. *Nat Rev Immunol* 2003 Dec;3(12):984-93.

3. Zelante T, et al. IL-17/Th17 in anti-fungal immunity: what's new? *Eur J Immunol* 2009 Mar;39(3):645-8.

4. Tato CM, et al. Immunology: what does it mean to be just 17? *Nature* 2006 May 11;441(7090):166-8.

5. Hussaarts L, et al. Priming dendritic cells for th2 polarization: lessons learned from helminths and implications for metabolic disorders. *Front Immunol* 2014;5:499.

6. Mathieson W, et al. A comparative proteomic study of the undeveloped and developed Schistosoma mansoni egg and its contents: the miracidium, hatch fluid and secretions. *Int J Parasitol* 2010 Apr;40(5):617-28.

7. Everts B, et al. Omega-1, a glycoprotein secreted by Schistosoma mansoni eggs, drives Th2 responses. *J Exp Med* 2009 Aug 3;206(8):1673-80.

8. Steinfelder S, et al. The major component in schistosome eggs responsible for conditioning dendritic cells for Th2 polarization is a T2 ribonuclease (omega-1). *J Exp Med* 2009 Aug 3;206(8):1681-90.

9. Everts B, et al. Schistosome-derived omega-1 drives Th2 polarization by suppressing protein synthesis following internalization by the mannose receptor. *J Exp Med* 2012 Sep 24;209(10):1753-67, S1.

10. Le NF, et al. Profiling changes in gene expression during differentiation and maturation of monocyte-derived dendritic cells using both oligonucleotide microarrays and proteomics. *J Biol Chem* 2001 May 25;276(21):17920-31.

11. Richards J, et al. Integrated genomic and proteomic analysis of signaling pathways in dendritic cell differentiation and maturation. *Ann N Y Acad Sci* 2002 Dec;975:91-100.

12. Gundacker NC, et al. Cytoplasmic proteome and secretome profiles of differently stimulated human dendritic cells. *J Proteome Res* 2009 Jun;8(6):2799-811.

13. Ferret-Bernard S, et al. Proteomic profiling reveals that Th2-inducing dendritic cells stimulated with helminth antigens have a 'limited maturation' phenotype. *Proteomics* 2008 Mar;8(5):980-93.

14. Ferret-Bernard S, et al. Plasma membrane proteomes of differentially matured dendritic cells identified by LC-MS/MS combined with iTRAQ labelling. *J Proteomics* 2012 Jan 4;75(3):938-48.

15. Ferreira GB, et al. Protein-induced changes during the maturation process of human dendritic cells: A 2-D DIGE approach. *Proteomics Clin Appl* 2008 Sep;2(9):1349-60.

16. Pereira SR, et al. Changes in the proteomic profile during differentiation and maturation of human monocyte-derived dendritic cells stimulated with granulocyte macrophage colony stimulating factor/interleukin-4 and lipopolysaccharide. *Proteomics* 2005 Apr;5(5):1186-98.

17. Richards J, et al. Integrated genomic and proteomic analysis of signaling pathways in dendritic cell differentiation and maturation. *Ann N Y Acad Sci* 2002 Dec;975:91-100.

18. Gundacker NC, et al. Cytoplasmic proteome and secretome profiles of differently stimulated human dendritic cells. *J Proteome Res* 2009 Jun;8(6):2799-811.

19. Palmblad M, et al. A novel mass spectrometry cluster for high-throughput quantitative proteomics. *J Am Soc Mass Spectrom* 2010 Jun;21(6):1002-11.

20. Johansson A, et al. Identification of genetic variants influencing the human plasma proteome. *Proc Natl Acad Sci U S A* 2013 Mar 19;110(12):4673-8.

21. Martinez-Pomares L. The mannose receptor. *J Leukoc Biol* 2012 Dec;92(6):1177-86.

4

22. Kolter T, et al. Principles of lysosomal membrane digestion: stimulation of sphingolipid degradation by sphingolipid activator proteins and anionic lysosomal lipids. *Annu Rev Cell Dev Biol* 2005;21:81-103.

23. Katunuma N, et al. Insights into the roles of cathepsins in antigen processing and presentation revealed by specific inhibitors. *Biol Chem* 2003 Jun;384(6):883-90.

24. Nigro P, et al. Cyclophilin A: a key player for human disease. *Cell Death Dis* 2013;4:e888.

25. Termeer C, et al. Targeting dendritic cells with CD44 monoclonal antibodies selectively inhibits the proliferation of naive CD4+ T-helper cells by induction of FAS-independent T-cell apoptosis. *Immunology* 2003 May;109(1):32-40.

26. Everts B, et al. Helminths and dendritic cells: sensing and regulating via pattern recognition receptors, Th2 and Treg responses. *Eur J Immunol* 2010 Jun;40(6):1525-37.

27. Ferreira GB, et al. Understanding dendritic cell biology and its role in immunological disorders through proteomic profiling. *Proteomics Clin Appl* 2010 Feb;4(2):190-203.

28. Alvarez D, et al. Mechanisms and consequences of dendritic cell migration. *Immunity* 2008 Sep 19;29(3):325-42.

29. Matsue H, et al. Generation and function of reactive oxygen species in dendritic cells during antigen presentation. *J Immunol* 2003 Sep 15;171(6):3010-8.

30. Yamada H, et al. LPS-induced ROS generation and changes in glutathione level and their relation to the maturation of human monocyte-derived dendritic cells. *Life Sci* 2006 Jan 25;78(9):926-33.

31. Rivollier A, et al. High expression of antioxidant proteins in dendritic cells: possible implications in atherosclerosis. *Mol Cell Proteomics* 2006 Apr;5(4):726-36.

32. Yamakita Y, et al. Fascin1 promotes cell migration of mature dendritic cells. *J Immunol* 2011 Mar 1;186(5):2850-9.

33. Buhligen J, et al. Lysophosphatidylcholine-mediated functional inactivation of syndecan-4 results in decreased adhesion and motility of dendritic cells. *J Cell Physiol* 2010 Nov;225(3):905-14.

34. Rescigno M, et al. Dendritic cell survival and maturation are regulated by different

35. Ferreira GB, et al. Protein-induced changes during the maturation process of human dendritic cells: A 2-D DIGE approach. *Proteomics Clin Appl* 2008 Sep;2(9):1349-60.

36. Srivastava P. Roles of heat-shock proteins in innate and adaptive immunity. *Nat Rev Immunol* 2002 Mar;2(3):185-94.

37. Fleckner J, et al. Differential regulation of the human, interferon inducible tryptophanyl-tRNA synthetase by various cytokines in cell lines. *Cytokine* 1995 Jan;7(1):70-7.

38. Mellor AL, et al. IDO expression by dendritic cells: tolerance and tryptophan catabolism. *Nat Rev Immunol* 2004 Oct;4(10):762-74.

39. Almawi WY, et al. Clinical and mechanistic differences between FK506 (tacrolimus) and cyclosporin A. *Nephrol Dial Transplant* 2000 Dec;15(12):1916-8.

40. Pearce EL, et al. Metabolic pathways in immune cell activation and quiescence. *Immunity* 2013 Apr 18;38(4):633-43.

41. Pearce EJ, et al. Dendritic cell metabolism. *Nat Rev Immunol* 2014 Dec 23;15(1):18-29.

42. Tchorzewski M. The acidic ribosomal P proteins. *Int J Biochem Cell Biol* 2002 Aug;34(8):911-5.

43. Constant S, et al. Extent of T cell receptor ligation can determine the functional differentiation of naive CD4+ T cells. *J Exp Med* 1995 Nov 1;182(5):1591-6.

44. Hosken NA, et al. The effect of antigen dose on CD4+ T helper cell phenotype development in a T cell receptor-alpha beta-transgenic model. *J Exp Med* 1995 Nov 1;182(5):1579-84.

45. van Panhuys N, et al. T-Cell-Receptor-Dependent Signal Intensity Dominantly Controls CD4(+) T Cell Polarization In Vivo. *Immunity* 2014 Jul 17;41(1):63-74.

46. Hussaarts L, et al. Rapamycin and omega-1: mTOR-dependent and -independent Th2 skewing by human dendritic cells. *Immunol Cell Biol* 2013 Aug;91(7):486-9.

47. Dutch Federation of Medical Scientific Societies. Dutch Federation of Medical Scientific Societies. www fedra org 2013 [cited 2013 Sep 17];Available from: URL: www.fedra.org

48. Pedrioli PG, et al. A common open representation of mass spectrometry data

signaling pathways. *J Exp Med* 1998 Dec 7;188(11):2175-80.

and its application to proteomics research. *Nat Biotechnol* 2004 Nov;22(11):1459-66.

49. Wolstencroft K, et al. The Taverna workflow suite: designing and executing workflows of Web Services on the desktop, web or in the cloud. *Nucleic Acids Res* 2013 Jul;41(Web Server issue):W557-W561.

50. Craig R, et al. TANDEM: matching proteins with tandem mass spectra. *Bioinformatics* 2004 Jun 12;20(9):1466-7.

51. Keller A, et al. A uniform proteomics MS/MS analysis platform utilizing open XML file formats. *Mol Syst Biol* 2005;1:2005.

52. Palmblad M, et al. Chromatographic alignment of LC-MS and LC-MS/MS datasets by genetic algorithm feature extraction. *J Am Soc Mass Spectrom* 2007 Oct;18(10):1835-43.

53. Keller A, et al. Empirical statistical model to estimate the accuracy of peptide identifications made by MS/MS and database search. *Anal Chem* 2002 Oct 15;74(20):5383-92.

54. Mi H, et al. PANTHER in 2013: modeling the evolution of gene function, and other gene attributes, in the context of phylogenetic trees. *Nucleic Acids Res* 2013 Jan;41(Database issue):D377-D386.

55. Mi H, et al. Large-scale gene function analysis with the PANTHER classification system. *Nat Protoc* 2013 Aug;8(8):1551-66.

56. Warde-Farley D, et al. The GeneMANIA prediction server: biological network integration for gene prioritization and predicting gene function. *Nucleic Acids Res* 2010 Jul;38(Web Server issue):W214-W220.
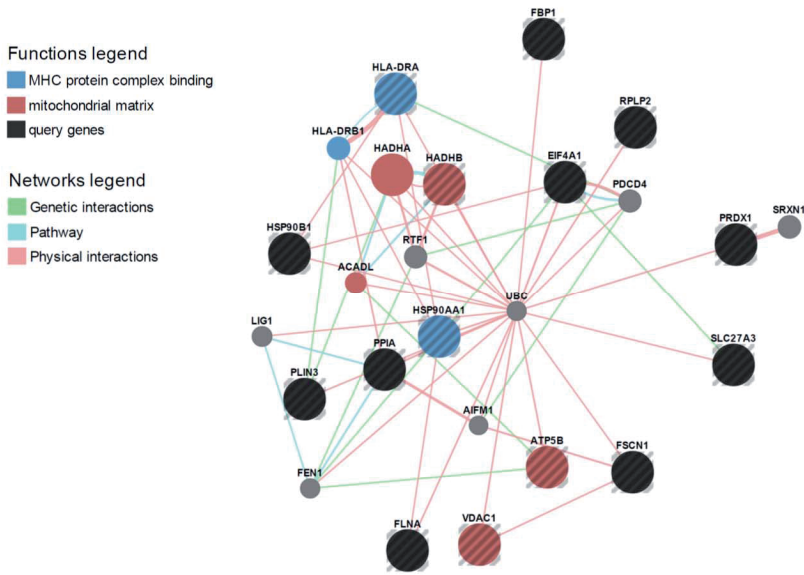
4

SUPPLEMENTAL DATA

Figure S1. Network analysis of 6h SEA-response proteins. Monocyte-derived DCs were pulsed with LPS in the presence of SEA or omega-1, and protein expression was analyzed by LC-FTICRMS. For GeneMANIA analysis, all 6h SEA-responsive proteins with P<0.05, and those proteins with P<0.1 and a fold change of <0.67 or >1.5, were included. Black and/or striped nodes represent genes of which the proteins were differentially expressed (query genes); grey nodes represent associated genes added by GeneMANIA. Colored nodes highlight significantly enriched Gene Ontologies.
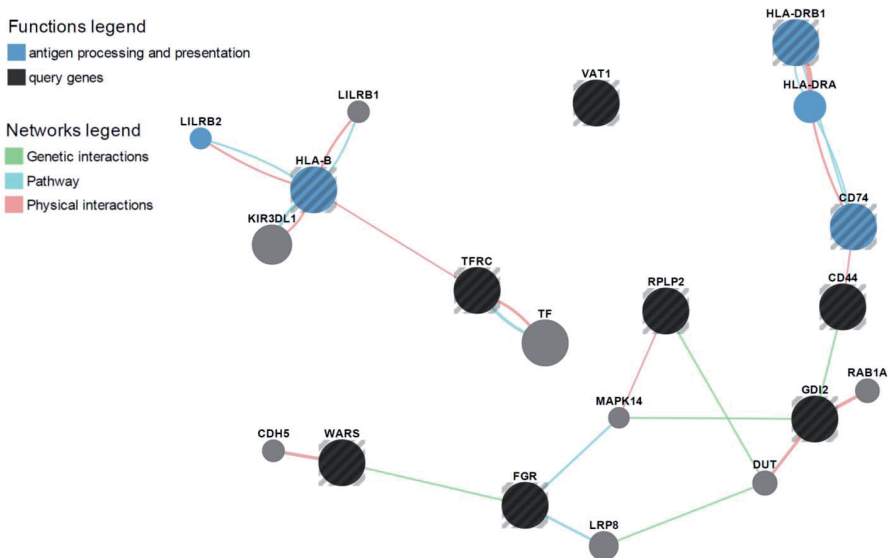
Figure S3. Network analysis of 6h omega-1-response proteins. Monocyte-derived DCs were pulsed and analyzed as describe for figure S1. For GeneMANIA analysis, all 6h omega-1-responsive proteins with P<0.05, and those proteins with P<0.1 and a fold change of <0.67 or >1.5, were included. Black and/or striped nodes represent genes of which the proteins were differentially expressed (query genes); grey nodes represent associated genes added by GeneMANIA. Colored nodes highlight significantly enriched Gene Ontologies.
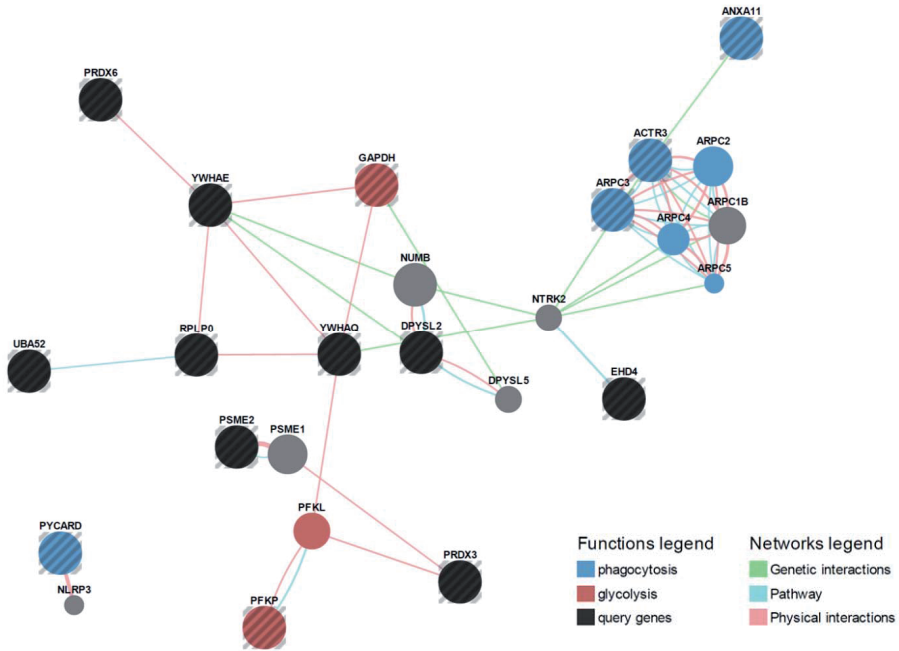
◄ **Figure S2. Network analysis of 32h SEA-response proteins.** Monocyte-derived DCs were pulsed and analyzed as describe for figure S1. For GeneMANIA analysis, all 32h SEA-responsive proteins with P<0.05, and those proteins with P<0.1 and a fold change of <0.67 or >1.5, were included. Black and/or striped nodes represent genes of which the proteins were differentially expressed (query genes); grey nodes represent associated genes added by GeneMANIA. Colored nodes highlight significantly enriched Gene Ontologies.

Table S1. Differentially expressed proteins included for GeneMANIA analysis.

Accession	Gene Name	Fold Change	P-value
SEA-induced, 6 hours			
P62937	PPIA	11.27	0.012
P14625	HSP90B1	4.14	0.039
P06576	ATP5B	3.44	0.075
P60842	EIF4A1	3.21	0.042
P07900	HSP90AA1	2.98	0.019
P01903	HLA-DRA	2.39	0.056
P21333	FLNA	2.07	0.091
Q06830	PRDX1	1.90	0.062
P55084	HADHB	1.79	0.093
Q16658	FSCN1	1.74	0.041
P05387	RPLP2	1.71	0.066
P09467	FBP1	1.54	0.074
O60664	PLIN3	1.36	0.035
P21796	VDAC1	0.78	0.048
Q5K4L6	SLC27A3	0.77	0.005
SEA-induced, 32 hours			
P05387	RPLP2	2,27	0,006
P50395	GDI2	1,60	0,093
Q99536	VAT1	1,59	0,028
P04229	HLA-DRB1	0,70	0,018
P04233	CD74	0,69	0,020
P09769	FGR	0,68	0,009
P16070	CD44	0,63	0,023
P23381	WARS	0,60	0,004
P02786	TFRC	0,56	0,002
P30464	HLA-B	0,45	0,003
Omega-1-induced, 6 hours			
P30048	PRDX3	4.03	0.036
Q9ULZ3	PYCARD	2.08	0.074
P05388	RPLP0	1.86	0.021
O15145	ARPC3	1.80	0.052
P30041	PRDX6	1.77	0.020
Q01813	PFKP	1.65	0.006
P61158	ACTR3	1.61	0.038
P27348	YWHAQ	1.46	0.014
Q9UL46	PSME2	1.43	0.005
Q9H223	EHD4	1.42	0.020

Table S1. Differentially expressed proteins included for GeneMANIA analysis. (*Continued*)

Accession	Gene Name	Fold Change	P-value
Q16555	DPYSL2	1.24	0.022
P62258	YWHAE	1.16	0.010
P62987	UBA52	0.83	0.041
P04406	GAPDH	0.72	0.043
P50995	ANXA11	0.72	0.043
Omega-1-induced, 32 hours			
P55084	HADHB	2.52	0.045
P63104	YWHAZ	2.33	0.035
P60842	EIF4A1	2.30	0.086
P50502	ST13	2.05	0.024
P30041	PRDX6	2.02	0.020
Q99536	VAT1	1.53	0.016
P06753	TPM3	1.43	0.049
P29692	EEF1D	1.35	0.001
P29966	MARCKS	0.58	0.015
P04179	SOD2	0.52	0.006
P02786	TFRC	0.49	0.002
P30504	HLA-C	0.47	0.019
P16070	CD44	0.47	0.002
P30464	HLA-B	0.40	0.002
Q9Y3Z3	SAMHD1	1.70	0.070
P27824	CANX	2.64	0.047
P05387	RPLP2	4.63	0.013
P30508	HLA-C	0.63	0.012
P17900	GM2A	0.65	0.026
P62987	UBA52	0.70	0.025
P07339	CTSD	0.73	0.036
P07858	CTSB	0.74	0.029
Q9BQE5	APOL2	0.76	0.031
P80723	BASP1	0.76	0.042

4